11th *International Congress on Engineered Material Platforms for Novel Wave Phenomena - Metamaterials 2017*
Marseille, France, Aug. 28th - Sept. 2nd 2017

PT Symmetry breaking in graphene-comprising photonic devices

D. Chatzidimitriou[1], **A. Pitilakis**[1] **and E. E. Kriezis**[1]

[1]Aristotle University of Thessaloniki, Department of Electrical & Computer Engineering, University Campus, 54124, Thessaloniki, Greece
dchatzid@auth.gr

Abstract **– The concept of PT Symmetry has recently received considerable attention as a novel approach for manipulating light in nanophotonic devices. We investigate graphene as a means of probing passive PT Symmetry in a photonic coupler at the telecom wavelength and show that it can be used for the design of switching elements. We present passive PT dynamics, emphasising on properties for a compact/low-loss design, and note appropriate biasing conditions for graphene. Finally, various graphene configurations are investigated to highlight polarisation dependent symmetry breaking.**

I. Introduction

The most well established Parity-Time Symmetry (PT Symmetry) framework in photonics involves two coupled photonic elements with balanced gain and loss so that the refractive index profile obeys the relation $n(x) = n^*(-x)$ [1], $(*)$ denoting complex conjugation. Equally noteworthy is the passive application of PT Symmetry [2], where gain/loss is substituted by high/low losses. Such schemes, both active and passive, are the object of intense theoretical and experimental research, demonstrating diverse photonic functionalities from switching to non-reciprocal behaviour [3]. Graphene's unique band structure enables the implementation of passive PT Symmetry concepts in nanophotonic waveguides as one of graphene's key properties is the ability to tune its electric conductivity by means of externally applied bias-voltage.

II. Framework

A. Passive PT Symmetry

We employ the commonly used coupled mode theory (CMT) model of two identical coupled waveguides where modes differ only in their loss coefficients: α_1, α_2. The eigenvalues of the system provide the propagation constants of the supported super-modes:

$$\beta = \beta_0 - j\frac{\alpha_1 + \alpha_2}{2} \pm \sqrt{|\kappa|^2 - \left(\frac{\Delta\alpha}{2}\right)^2}, \tag{1}$$

where β_0 is the uncoupled propagation constant in the absence of loss/gain, $\Delta\alpha = \alpha_1 - \alpha_2$, $|\kappa| = \pi/(2L_{\text{c}})$ is the magnitude of the coupling coefficient and L_{c} is the coupling length. Eq. (1) exhibits the existence of exceptional points (EPs): critical values in the parameter space at which the eigenvalues coalesce. For this two-mode configuration the single EP is identified at $|\Delta\alpha| = 2|\kappa|$ while for $|\Delta\alpha| > 2|\kappa|$ the system enters the so called broken PT phase. At this phase, as $|\Delta\alpha|$ grows, super-modes experience increasing/decreasing losses, asymptotically approaching their un-coupled β values. Therefore, only the low-loss super-mode effectively survives. Note that, unlike active PT Symmetry, $\Delta\alpha$ must be sufficiently higher than $2|\kappa|$ in order to achieve low-loss transmission in the broken phase. To that end, we set $\alpha_1 = 0$ and assume that α_2 can be varied between the values of α_L and α_H, corresponding to operation below and above the EP, respectively. For power injection in the lossless waveguide and coupler length of L_{c}, starting from Eq. (1) we approximate the values of α_{H}, α_{L} and L_{c} needed to achieve transmission with insertion losses (IL) below an arbitrary level A :

$$\begin{array}{lcl} \alpha_{\text{L}} L_{\text{c}} & < & A, \\ \alpha_{\text{H}} L_{\text{c}} & > & (A^2 + \pi^2)/(2A), \end{array} \tag{2}$$

where $A = A_{\text{dB}}/4.343$ and we assumed that propagation losses coincide with those of the low-loss super-mode. Eq. (2) underlines the fact that increasing α_{L} and α_{H} ensues the same performance, if we decrease L_{c} accordingly. Thus, as long as losses only slightly perturb the photonic modes, increasing α_{H} leads to a more compact design. Finally, keeping L_{c} constant and increasing α_{H} improves transmission.

B. Graphene Conductivity

Graphene's surface conductivity can be tuned by changing its chemical potential μ_{c} [4], a quantity that in graphene coincides with the Fermi level. For μ_{c} greater than half the photon energy $\hbar\omega/2$, interband electron transitions are blocked and graphene is rendered almost transparent. At a wavelength of $1.55\ \mu\text{m}$ the critical value is roughly $\mu_{\text{c}} = 0.4$ eV.

According to Eq. (2), compact design requires multiple monolayers or few-layer graphene (FLG) stacks. FLG consists of a stack of $N < 9$ monolayers and its linear conductivity is N times that of a monolayer, rendering α_{H} and α_{L} proportional to N. In this case, the impact on the real part of the effective refractive index (n_{eff}) is not negligible if arbitrarily biased, as seen in Fig. 1(b). To overcome this, μ_{c} is set to 0.2 eV and 0.5 eV, leading to a surface conductivity of $187.2 + 6j\ \mu\text{S}$ and $13.8 - 16.8j\ \mu\text{S}$, respectively, for $N = 3$.

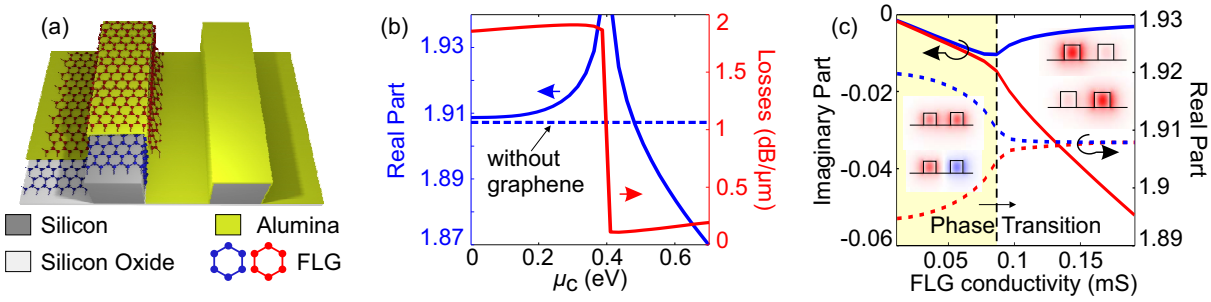

Fig. 1: (a) PT Symmetric coupler with a FLG-alumina-FLG stack. (b) Effective refractive index (n_{eff}) vs. μ_{c} of the TE mode in an uncoupled waveguide. (c) n_{eff} of the coupler's TE super-modes vs. FLG surface conductivity. The minimum/maximum conductivity values correspond to $\mu_{\text{c}} = 0.5$ and 0.2 eV, respectively. (insets) Super-mode profiles below and above the EP.

III. Application

The photonic coupler is theoretically investigated using a finite element method (FEM) formulation for the eigenmode analysis of the waveguide cross-section. The proposed device [Fig. 1(a)] consists of two air-clad silicon ($n_{\text{Si}} = 3.45$) strip waveguides, 320 nm wide and 280 nm thick, on top of a silicon oxide ($n_{\text{SiO}_2} = 1.48$) substrate. The waveguides are separated by a 400 nm wide gap. A stack of two FLG sheets ($N = 3$), with a 7 nm layer of Al_2O_3 ($n_{\text{Al}_2\text{O}_3} = 1.66$) in between, is used to coat one of the waveguides, whilst the other is only coated by alumina, also of 7 nm thickness. Meticulously choosing dimensions for optimal overlap of the TE mode with FLG, we attain a greatly enhanced performance compared to previously reported designs [5]. Furthermore, device length is more than halved from what it was reported in [6] while also facilitating fabrication. The improved performance, is attributed to the strong interaction of graphene with the longitudinal component of the electric field.

A. Switching

Power injected in the lossless waveguide is switched by tuning the operation of the coupler below or above the EP [Fig. 1(c)]. Below the EP (cross state), super-modes coincide with the symmetric/anti-symmetric pair and the device operates as a conventional coupler. Above the EP (bar state), super-modes are mainly confined to the individual waveguides so that one experiences far greater losses than the other, as shown in the inset of Fig. 1(c). Therefore, only the low-loss super-mode survives and power principally exits from the lossless waveguide. From Eq. (2) we estimate that, for IL < 3 dB and $L_{\text{c}} = 31\ \mu\text{m}$, approximately 2 dB/$\mu$m absorption is required, which is satisfied according to Fig. 1(b). Evaluation by FEM-backed CMT calculations set the IL of the switch at 2 dB

and 2.7dB at the cross and bar state, respectively. Injection in the lossy waveguide results into heavy losses so the configuration can only operate as a 1×2 switch.

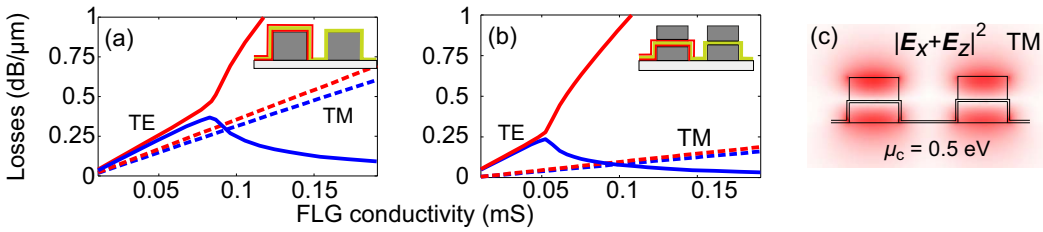

Fig. 2: Loss coefficient of the TE (solid) and TM (dashed) super-modes vs. FLG surface conductivity. The minimum/maximum conductivity values correspond to $\mu_c = 0.5$ and 0.2 eV, respectively. Placement of graphene is (a) on top or (b) in the middle of the waveguide. (c) TM symmetric super-mode of the main field components parallel to the FLG stacks. Waveguides in (b)-(c) are 310 nm wide and 360 nm thick. (insets) Graphene placement.

B. Polarisation dependent switching

Polarisation dependent switching requires that either losses or coupling strength are adequately differentiated with respect to polarisation. In our design, TE and TM polarisations exhibit distinct PT Symmetry breaking points due to their different coupling lengths. Consequently, since the TM mode has a much lower L_c, it is not switched for $\mu_c = 0.2$ eV but simply experiences high losses, as depicted in Fig. 2(a).

Graphene interacts with electromagnetic radiation polarised parallel to the sheet, therefore, when graphene is placed in the middle of the waveguide, the TM polarised mode will be almost insensitive to the conductivity changes of the graphene layers. Thus, in contrast to the previous scenario, the TM mode will not experience a PT phase transition due to inefficient overlap with the graphene layers,[(inset Fig. 2(b)]. For a clear demonstration, as well as placing graphene in the middle of the waveguide, we adjust the waveguide dimensions so that both polarisations have $L_c \sim 50\ \mu\text{m}$ and plot the results in Fig. 2(b).

IV. Conclusions

We have demonstrated that FLG can be employed for effectuating passive PT symmetry breaking, which in turn provides a switching mechanism. It was highlighted that proper manipulation of graphene properties is essential for achieving high performance and compact design. Finally, we exhibited polarization dependent PT Symmetric breaking stemming from graphene's anisotropic surface conductivity.

References

[1] C.E. Rüter, K.G. Makris, R. El-Ganainy, D.N. Christodoulides, M. Segev and D. Kip, "Observation of paritytime symmetry in optics," *Nature Physics,* vol. 6, pp. 192-195, 2010.
[2] A. Guo, G.J. Salamo, D. Duchesne, R. Morandotti, M. Volatier-Ravat, V. Aimez, G.A. Siviloglou and D.N. Christodoulides, "Observation of PT-Symmetry breaking in Complex Optical Potentials," *Physical Review Letters,* vol. 103, no. 9, p. 093902, 2009.
[3] S.V. Suchkov, A.A. Sukhorukov, J. Huang, S.V. Dmitriev, C. Lee, Y.S. Kivshar, "Nonlinear switching and solitons in PT-symmetric photonic systems," *Laser & Photonics Reviews,* vol. 10, no. 2, pp. 177-213, 2016.
[4] T. Gu, N. Petrone, J.F. McMillan, A. van der Zande, M. Yu, G.Q. Lo, D.L. Kwong, J. Hone and C.W. Wong, "Regenerative oscillation and four-wave mixing in graphene optoelectronics," *Nature Photonics,* vol. 6, pp. 554-559, 2012.
[5] M. Liu, X. Yin, and X. Zhang, "Double-layer graphene optical modulator," *Nano Letters,* vol. 12, pp. 1482-1485, 2012.
[6] A. Locatelli, A. Capobianco, M. Midrio, S. Boscolo and C. De Angelis, "Graphene-assisted control of coupling between optical waveguides," *Optics Express,* vol. 20, no. 27, pp. 28479-28484, 2012.

Acknowledgement

This work was supported by the Aristotle University of Thessaloniki Research Committee through the 2015 "Excellence Grant" for PhD candidates.